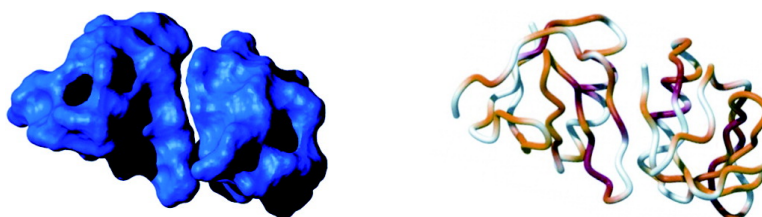# Large-Scale Millisecond Intersubunit Dynamics in the B Subunit Homopentamer of the Toxin Derived from *Escherichia coli* O157

Anna Yung, W. Bruce Turnbull, Arnout P. Kalverda, Gary S. Thompson, Steve W. Homans, Pavel Kitov, and David R. Bundle

More About This Article

Additional resources and features associated with this article are available within the HTML version:

- Supporting Information
- Links to the 1 articles that cite this article, as of the time of this article download
- Access to high resolution figures
- Links to articles and content related to this article
- Copyright permission to reproduce figures and/or text from this article

View the Full Text HTML

Large-Scale Millisecond Intersubunit Dynamics in the B Subunit Homopentamer of the Toxin Derived from *Escherichia coli* O157

Anna Yung,[†] W. Bruce Turnbull,[†] Arnout P. Kalverda,[†] Gary S. Thompson,[†] Steve W. Homans,*,[†] Pavel Kitov,[‡] and David R. Bundle[‡]

Contribution from the Astbury Centre for Structural Molecular Biology, School of Biochemistry and Molecular Biology, University of Leeds, Leeds LS2 9JT, United Kingdom, and the Chemistry Department, University of Alberta, Edmonton, Canada T6G 2G2

Received June 17, 2003; E-mail: s.w.homans@leeds.ac.uk

Abstract: We report here solution NMR relaxation measurements that show millisecond time-scale intersubunit dynamics in the homopentameric B subunit (VTB) of the toxin derived from *Escherichia coli* O157. These data are consistent with interconversion between an axially symmetric form and a low-abundance (~10%, 45 °C) higher energy form. The higher energy state is depopulated on binding of a novel bivalent analogue (P^k dimer) of the natural carbohydrate acceptor globotriaosylceramide. The isothermal titration calorimetry isotherm for the binding of P^k dimer to VTB is consistent with a five-site sequential binding model which assumes that cooperative effects arise through communication only between neighboring binding sites. The resulting thermodynamic parameters ($K_{a1} = 114 \pm 2.2$ M^{-1}, $K_{a2} = 283 \pm 4.5$ M^{-1}, $\Delta H_1° = -116.3 \pm 0.55$ kJ/mol, and $\Delta H_2° = -50.3 \pm 0.11$ kJ/mol) indicate favorable entropic cooperativity that has not previously been observed in multivalent systems.

Introduction

The toxin derived from *Escherichia coli* O157 is a member of the AB$_5$ class of cytotoxins,[1] comprising a catalytically active A subunit and a torus-shaped homopentameric B subunit (VTB) that binds to the cell-surface glycolipid globotriaosylceramide (Gb$_3$) in a multivalent manner.[2−4] The crystal structure of the B subunit shows similar intermonomer β-sheet interactions between $\beta2$ of monomer *n* and $\beta6$ of monomer *n* + 1, except between two monomers, resulting from a screw component of about 0.13 nm in the 5-fold rotation axis of the pentamer.[5] In contrast, NMR measurements suggest a dominant conformer that is a symmetric homopentamer in solution,[6] consistent with a single set of cross-peaks in ^{1}H−^{15}N correlation spectra. However, ^{1}H−^{15}N correlation spectra recorded on the protein in the presence of a 5-fold molar excess of the bivalent inhibitor P^k dimer, which is a bridged dimer analogue of the Gb$_3$ carbohydrate,[7] are characterized by a reduction of resonance line widths for a number of resonances. These data suggest an exchange contribution to the line widths of the B subunit in the
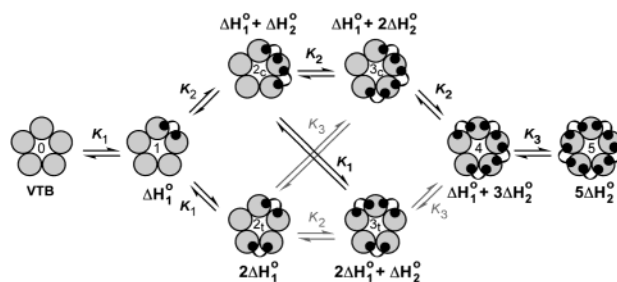

Figure 1. Sequential binding model showing up to five copies of the bivalent ligand cross-linking VTB subunits. The eight possible states are designated as 0, 1, 2$_{cis}$, 2$_{trans}$, 3$_{cis}$, 3$_{trans}$, 4, and 5, and total enthalpy changes for each bound state relative to state 0 are indicated. Only seven (black equilibrium arrows) of the 10 stepwise binding constants are required to describe the system fully.

absence of P^k dimer, which accordingly was probed by use of NMR relaxation dispersion measurements.[8−10] Here we show that the exchange contribution to the line widths can be interpreted in terms of fast exchange between a symmetric conformation and a minor conformer that may be related to that observed in the crystal structure. Consequently, binding of P^k dimer cannot be interpreted in terms of a simple two-state model but is consistent with a sequential binding model involving cooperative effects. These effects involve a positive entropic component to cooperativity that has not been observed previously in multivalent systems to our knowledge.

† University of Leeds.
‡ University of Alberta.
(1) Aktories, K., Ed. *ADP-ribosylating toxins*; Springer-Verlag: Berlin, 1992; Vol. 175.
(2) Lindberg, A. A.; Brown, J. E.; Stromberg, N.; Westlingryd, M.; Schultz, J. E.; Karlsson, K. A. *J. Biol. Chem.* **1987**, *262*, 1779−1785.
(3) Waddell, T.; Head, S.; Petric, M.; Cohen, A.; Lingwood, C. *Biochem. Biophys. Res. Commun.* **1988**, *152*, 674−679.
(4) Samuel, J. E.; Perera, L. P.; Ward, S.; O'Brien, A. D.; Ginsburg, V.; Krivan, H. C. *Infect. Immun.* **1990**, *58*, 611−618.
(5) Stein, P. E.; Boodhoo, A.; Tyrrell, G. J.; Brunton, J. L.; Read, R. J. *Nature* **1992**, *355*, 748−750.
(6) Richardson, J. M.; Evans, P. D.; Homans, S. W.; DonohueRolfe, A. *Nat. Struct. Biol.* **1997**, *4*, 190−193.
(7) Kitov, P. I.; Shimizu, H.; Homans, S. W.; Bundle, D. R. *J. Am. Chem. Soc.* **2003**, *125*, 3284−3294.

(8) Palmer, A. G.; Kroenke, C. D.; Loria, J. P. *Nucl. Magn. Reson. Biol. Macromol. B* **2001**, *339*, 204−238.
(9) Skrynnikov, N. R.; Mulder, F. A. A.; Hon, B.; Dahlquist, F. W.; Kay, L. E. *J. Am. Chem. Soc.* **2001**, *123*, 4556−4566.
(10) Mulder, F. A. A.; Mittermaier, A.; Hon, B.; Dahlquist, F. W.; Kay, L. E. *Nat. Struct. Biol.* **2001**, *8*, 932−935.

Experimental Section

All NMR and ITC experiments were performed in 100 mM sodium phosphate buffer, pH 6.0, and at a temperature of 45 °C. Dispersion profiles for each amide ^{15}N were acquired at proton resonance frequencies of 500 and 750 MHz as described[9] and fitted to the appropriate equation for a two-site process on either fast[11] or all[12] exchange time scales by use of software kindly provided by Professor Art Palmer (Columbia University). The relevant exchange regime was determined by derivation of the parameter α from the exchange contribution to the line width (R_{ex}) at 500 and 750 MHz, as described,[13] and the fast exchange equation was used for $\alpha > 1.5$. The resulting values of the exchange rate k_{ex} lay within a relatively narrow range ($\sim$900 ± 400 s^{-1}), indicative of a single concerted exchange process. Subsequently each profile was fitted with a single average value of k_{ex} (1000 s^{-1}), giving a per-residue value of the exchange contribution to the line width $R_{ex} = p_a p_b \Delta\omega^2/k_{ex}$, with the equation appropriate for fast exchange, or $p_a p_b$, $\Delta\omega$, and k_{ex} with the equation appropriate for all exchange regimes.[10] The average value of $p_a p_b$ derived from the latter was used to calculate $\Delta\omega$ in the fast exchange regime from R_{ex}. The value of $\Delta\omega$ at each site was also evaluated for both the ground-state and putative excited-state conformations by the SHIFTS density functional approach[14] (http://www.scripps.edu/case/qshifts/qshifts.htm). NMR titration of P^k dimer binding was performed with ^{15}N-enriched VTB at an initial B-subunit concentration of 0.8 mM. ^{1}H chemical shifts were measured directly from a series of ^{1}H,^{15}N heteronuclear single quantum coherence (HSQC) spectra recorded at protein:ligand ratios up to 1:10 (based on binding sites). Data were fitted to a simple two-state binding model and to a cooperative binding model by use of the Hill equation:

$$\frac{f}{(1-f)} = K[A]^n$$

where f is the fraction of sites bound, K is a constant (not the binding constant for one ligand), n is the Hill coefficient (which varies from 1 for no cooperativity to N for all-or-none binding of N ligands), and [A] is the concentration of free ligand at equilibrium. Isothermal titration calorimetry (ITC) was conducted in a MicroCal VP−ITC unit, making 70 consecutive additions of 175 nmol of the bivalent ligand to a solution of VTB with an initial B-subunit concentration of 0.79 mM. VTB subunit concentration was calculated from its UV absorbance at 280 nm with a molar extinction coefficient of 8370 L mol^{-1} cm^{-1}, and the ligand concentration was measured by ^{1}H NMR spectroscopy in the presence of 5 mM ethanol as an internal standard. The heat of dilution for the ligand was subtracted from the titration data, and the first data point was deleted to allow for diffusion of ligand across the syringe tip during equilibration. The data were fitted to a noninteracting one-site model provided by MicroCal or to a five-site sequential binding model (Figure 1)[15] which assumes that cooperative effects arise through communication only between neighboring binding sites:[16]

$$\Delta Q_{(i)} = \frac{[P]_t V_0 [\Delta x_1 \Delta H_1^{\circ} + \Delta x_{2c}(\Delta H_1^{\circ} + \Delta H_2^{\circ}) + \Delta x_{2t} 2\Delta H_1^{\circ} + \Delta x_{3c}(\Delta H_1^{\circ} + 2\Delta H_2^{\circ}) + \Delta x_{3t}(2\Delta H_1^{\circ} + \Delta H_2^{\circ}) + \Delta x_4(\Delta H_1^{\circ} + 3\Delta H_2^{\circ}) + \Delta x_5 5\Delta H_2^{\circ}]}{V_{inj(i)}[A]_{syr}}$$

where $\Delta Q_{(i)}$ is the change in heat on the ith injection (normalized with respect to moles of added ligand), $[P]_t$ is the total VTB *pentamer* concentration, V_0 is the effective cell volume, $V_{inj(i)}$ is the volume of the ith injection, $[A]_{syr}$ is the concentration of ligand in the syringe, ΔH_1° and ΔH_2° are stepwise enthalpy changes, and Δx_y is the change in molar fraction of the yth state (Figure 1) on the ith injection, for which

$$x_1 = 5K_1[A]/z \qquad\qquad x_{3t} = 5K_1^2 K_2 [A]^3/z$$

$$x_{2c} = 5K_1 K_2 [A]^2/z \qquad\qquad x_4 = 5K_1 K_2^3 [A]^4/z$$

$$x_{2t} = 5K_1^2 [A]^2/z \qquad\qquad x_5 = K_2^5 [A]^5/z$$

$$x_{3c} = 5K_1 K_2^2 [A]^3/z$$

where

$$z = 1 + 5K_1[A] + 5K_1 K_2[A]^2 + 5K_1^2[A]^2 + 5K_1 K_2^2[A]^3 + 5K_1^2 K_2[A]^3 + 5K_1 K_2^3[A]^4 + K_2^5[A]^5$$

wherein K_1 and K_2 are stepwise binding constants and [A] is the free ligand concentration, which is the root of the following polynomial for $0 \leq [A] \leq [A]_t$ (the total ligand concentration), as determined numerically by a bisection search:

$$0 = [A] - [A]_t + \frac{5[P]_t(K_1[A] + 2K_1 K_2[A]^2 + 2K_1^2[A]^2 + 3K_1 K_2^2[A]^3 + 3K_1^2 K_2[A]^3 + 4K_1 K_2^3[A]^4 + K_2^5[A]^5)}{1 + 5K_1[A] + 5K_1 K_2[A]^2 + 5K_1^2[A]^2 + 5K_1 K_2^2[A]^3 + 5K_1^2 K_2[A]^3 + 5K_1 K_2^3[A]^4 + K_2^5[A]^5}$$

Thus, K_1 and ΔH_1° are for ligand binding to an isolated site and K_2 and ΔH_2° are for ligand binding adjacent to an occupied site. Although a third association constant K_3 (for binding between two occupied sites) is required to complete the model, $K_1 K_3 = K_2 K_2$. Consequently, K_1 describes the first molecule of ligand to bind to a pentamer, whereas K_2 represents the average stepwise binding constant when all sites are occupied. The model was implemented in the Origin LabTalk scripting language in a manner analogous to that used by Sigurskjold[17] for his ITC displacement model.

Errors quoted are based on those determined by Origin during the fitting process. The improvements in fit for the Hill model and the sequential binding model, relative to the simple two-state models, were evaluated by F-tests. It was thus demonstrated, in all cases, that there was >95% probability that the improvement in fit was not simply a consequence of increasing the number of variable parameters in the fitting equations.
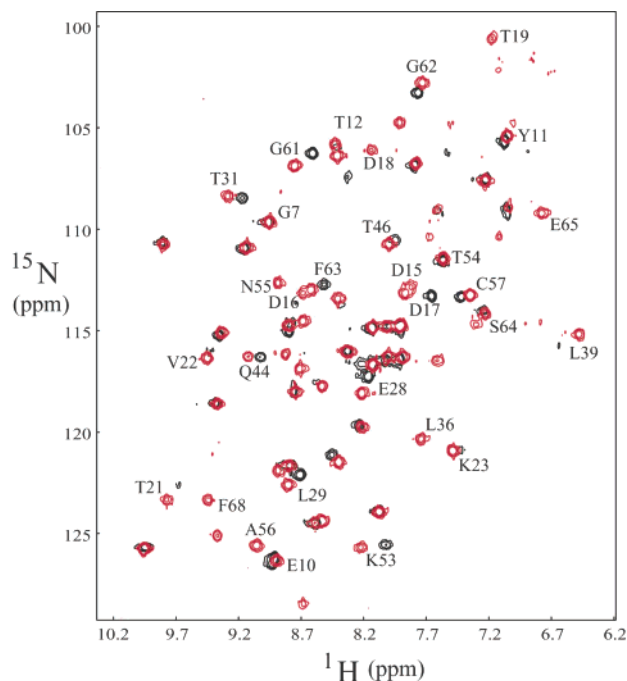
Figure 2. ^{15}N$-$^{1}H HSQC spectra of VTB in the absence (black contours) and presence (red contours) of bivalent inhibitor P^k dimer. Resonance assignments of residues that experience a shift on inhibitor binding are labeled. Note that in a number of instances (e.g., L39 to the right of the figure) the resonance is broadened to the limit of, or below, detection in the absence of inhibitor.

Results

^{1}H$-$^{15}N correlation spectra recorded on VTB in the absence and presence of a 5-fold molar excess of the bivalent inhibitor P^k dimer[7] are shown in Figure 2.

Initially, dispersion profiles were obtained for all assigned backbone amide ^{15}N resonances in the absence of P^k dimer at a field strength corresponding to a ^{1}H frequency of 500 MHz and at a sample temperature of 45 °C. Flat dispersion profiles were observed for many resonances, indicating that these are not sensitive to conformational exchange. However, a number of resonances in the vicinity of the $\beta2_n - \beta6_{n+1}$ interface exhibit significant relaxation dispersion (Figure 3a), namely, Tyr 11, Lys 13, Val 22, Lys 23, Gly 25, Thr 31, Leu 40, Val 50, and Phe 63, indicative of conformational exchange in this region that involves substantial changes in chemical shift.

At 35 °C, many of these resonances are too broad to obtain reliable dispersion profiles (data not shown), suggesting that the exchange regime at 45 °C is intermediate-fast. To determine the appropriate exchange regime for each site, relaxation dispersion profiles were also determined at 750 MHz (not shown), from which the parameter α was calculated[13] by using the relevant values of R_{ex} at 500 and 750 MHz. This was only possible for three residues (Tyr 11, Gly 25, and Phe 63, all of which possess α = 1.6 or greater) since the intensities of the remaining resonances were close to the noise floor at 750 MHz due to extreme exchange broadening. Consequently Tyr 11, Gly
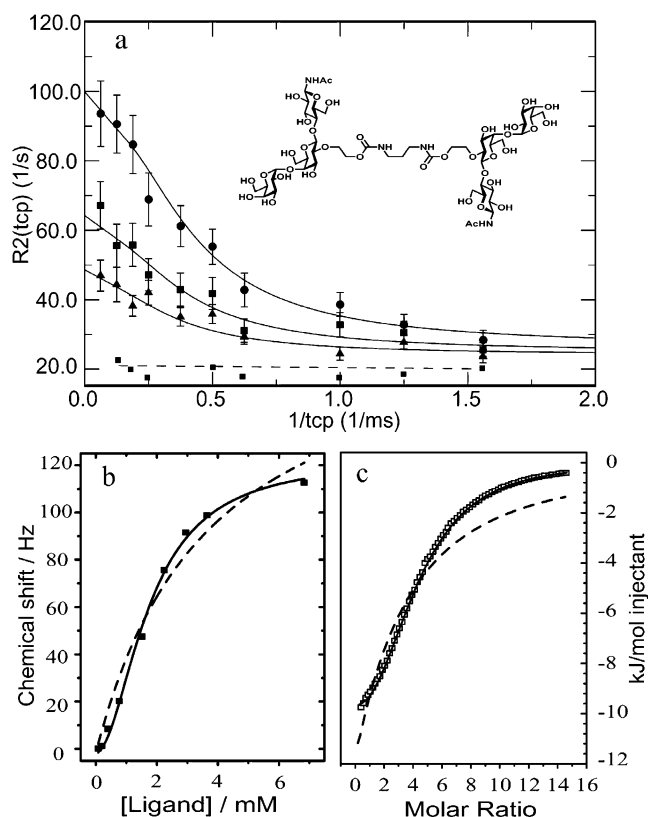
(11) Luz, Z.; Meiboom, S. *J. Chem. Phys.* **1963**, *39*, 366−370.
(12) Carver, J. P.; Richards, R. E. *J. Magn. Reson.* **1972**, *6*, 89−105.
(13) Millet, O.; Loria, J. P.; Kroenke, C. D.; Pons, M.; Palmer, A. G. *J. Am. Chem. Soc.* **2000**, *122*, 2867−2877.
(14) Xu, X. P.; Case, D. A. *J. Biomol. NMR* **2001**, *21*, 321−333.
(15) Schafer, D. E.; Thakur, A. K. *Cell Biophys.* **1982**, *4*, 25−40.
(16) Schoen, A.; Freire, E. *Biochemistry* **1989**, *28*, 5019−5024.
(17) Sigurskjold, B. W. *Anal. Biochem.* **2000**, *277*, 260−266.

Figure 3. (a) Typical ^{15}N relaxation dispersion profiles for the amide nitrogens of Val 50 (●), Val 22 (■), and Lys 23 (▲) in VTB. The relaxation dispersion profile for Val 50 in the presence of 5-fold molar excess of inhibitor P^k dimer (inset) is shown by the broken line. Solid lines represent the best fit to the data with the equation appropriate for all exchange time scales with $k_{ex} = 1000$ s^{-1}. (b) Titration of the ^{1}H^N chemical shift of Asp 17 in VTB with P^k dimer ligand. The broken line represents the best fit of the data to a simple two-state binding model with $K_a = 529 \pm 102$ M^{-1} and with the VTB:ligand stoichiometry fixed at 1:5, whereas the solid line represents the best fit to the Hill equation with $K = 1.76 \pm 0.1$ mM and $n = 1.90 \pm 0.15$ (see Experimental Section). (c) ITC binding isotherm for binding of P^k dimer to VTB. The broken line indicates the best fit of these data to a simple two-state binding model with $K_a = 159 \pm 13$ M^{-1} and with the VTB:ligand stoichiometry fixed at 1:5, whereas the solid line indicates the best fit to a sequential binding model with $K_{a1} = 114 \pm 2.2$ M^{-1}, $K_{a2} = 283 \pm 4.5$ M^{-1}, $\Delta H_1° = -116.3 \pm 0.55$ kJ/mol, and $\Delta H_2° = -50.3 \pm 0.11$ kJ/mol (see Experimental Section).

25, and Phe 63 were fit at two fields using the equation appropriate for fast exchange,[11] and the equation appropriate for all time-scale exchange[12] was used to fit the remaining residues at 500 MHz. The resulting values of the exchange rate k_{ex} lay within a relatively narrow range ($\sim900 \pm 400$ s^{-1}), indicative of a single concerted exchange process. Subsequently each profile was fitted with a single average value of $k_{ex} = 1000$ s^{-1} (Figure 3). In the fast-exchange limit this gives a per-residue value of the exchange contribution to the line width $R_{ex} = p_a p_b \Delta\omega^2/k_{ex}$, where p_a and p_b are the populations of the ground and excited states, respectively, and $\Delta\omega$ is the chemical shift difference between states.[10] In the intermediate exchange regime $p_a p_b$ and $\Delta\omega$ can be obtained independently, and thus $\Delta\omega$ was determined for residues in fast exchange from R_{ex} by using the average value of $p_a p_b$. Residues with a measurable R_{ex} are highlighted in the NMR-derived structure of the pentamer in Figure 4.

It can be seen that residues with the largest R_{ex} values are clustered at the interface between adjacent monomers, suggesting significant conformational exchange in this region of the

● $R_{ex} \geq 20/s$
● $R_{ex} = 10/s$
● $R_{ex} = 5/s$
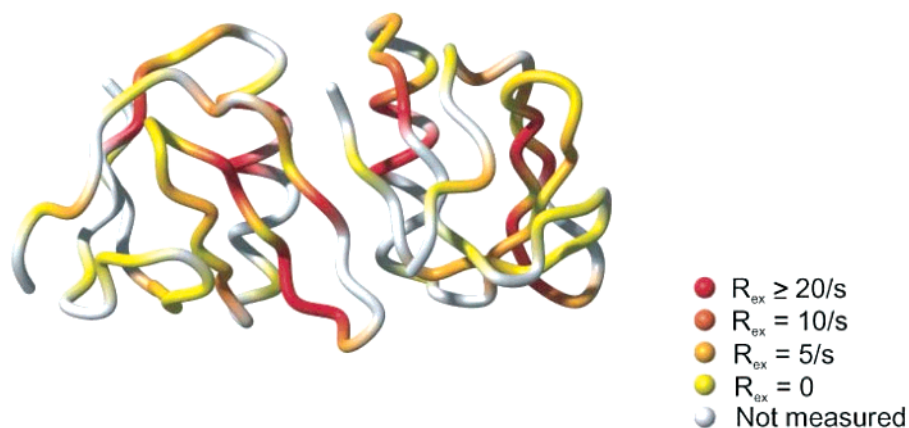● $R_{ex} = 0$
○ Not measured

Figure 4. (a) Relative orientation of two adjacent subunits in the VTB homopentamer corresponding with the axially symmetric conformation observed in solution. The figure is colored according to the exchange contribution (R_{ex}) to the R_2 relaxation of the amide ^{15}N of the relevant residue using the key as illustrated. Residues shaded white indicate that no resonance assignment is available or that the corresponding resonance is exchange-broadened below the limit of detection. This figure was prepared with the program MOLMOL.[18]

Table 1. Parameters Characterizing Millisecond Solution Dynamics in the B-Subunit of the Toxin Derived from *E. coli* O157, Derived from ^{15}N Relaxation Dispersion Experiments

residue	$\delta\omega$ ^{15}N (ppm) (exptl)^a	$\delta\omega$ ^{15}N (ppm) (theor)	population of excited state p_b(%)^a	$\chi^{2\,b}$
Tyr 11^c	1.0 ± 0.2	4.5	9.7	2.1
Lys 13	2.0 ± 1.3	3.2	11.5	0.4
Val 22	2.6 ± 1.5	5.3	9.6	0.7
Lys 23	1.9 ± 1.1	3.7	9.5	1.2
Gly 25^c	0.6 ± 0.1	1.0	9.7	1.8
Thr 31	1.3 ± 0.5		6.4	1.3
Leu 40	2.0 ± 0.8		7.5	1.2
Val 50	3.2 ± 1.2	3.8	13.7	0.9
Phe 63^c	0.82 ± 0.1		9.7	1.1

^{a} Values obtained by fitting with an average exchange rate $k_{ex} = 1000$ s^{-1} ^{b} Reduced χ^2 for the fitting of relaxation dispersion profiles (see text for details). ^{c} Data fitted to the equation for fast exchange time scales at two frequencies (500 and 750 MHz). Remaining sites are fitted to the equation for all exchange time scales at 500 MHz.

molecule. A possible candidate for this higher energy state is the asymmetric conformation observed in the crystal structure of the B-subunit, which exhibits significant differences from the NMR-derived structure in the region detected by the above relaxation dispersion measurements (Figure 4). Accordingly, we utilized a chemical shift prediction approach based on density functional theory described by Xu and Case[14] to calculate $\Delta\omega$ from the structures of the two states. Three of the nine residues for which R_{ex} values could be obtained (Thr 31, Leu 40, and Phe 63) had experimental ^{15}N shifts that were not bracketed by the theoretically derived values, which we attribute to the limitations of the prediction. These residues were consequently not included in this analysis. It can be seen from Table 1 that there is not a good correlation between experimental and theoretical shifts. However, the error in the measured values for sites in intermediate exchange is large, due to a shallow minimum in the fitting function for these sites. These errors, combined with unknown errors in the predicted values, render inconclusive the precise nature of the excited state.

In the presence of a 5-fold molar excess of the bivalent inhibitor P^k dimer, which has been shown to straddle binding sites in adjacent monomers,[7] all relaxation dispersion profiles were flat (Figure 3a), indicating that the higher energy form of the B subunit is depopulated on ligand binding. The affinity of P^k dimer was determined by titration into ^{15}N-enriched VTB

and acquisition of two-dimensional ^{15}N$-^1$H HSQC spectra at each ligand:protein ratio. The binding curve obtained by plotting the change in ^{1}H chemical shift of Asp 17 versus ligand concentration at 45 °C (Figure 3b) was fitted to a simple two-state binding model with $K_a = 529 \pm 102$ M^{-1}, but a much improved fit was obtained with a cooperative binding model described by the Hill equation with $K = 1.76 \pm 0.1$ mM and $n = 1.9 \pm 0.15$. Similarly, the higher precision binding data obtained from isothermal titration calorimetry experiments under the same conditions were not well-fitted to a simple two-state model (Figure 3c) but instead were consistent with a cooperative sequential binding model[15,16] with $K_{a1} = 114 \pm 2.2$ M^{-1}, $K_{a2} = 283 \pm 4.5$ M^{-1}, $\Delta H_1° = -116.3 \pm 0.55$ kJ/mol, and $\Delta H_2° = -50.3 \pm 0.11$ kJ/mol.

Discussion

The above data indicate that the B subunit homopentamer derived from *E. coli* O157 exists in solution in fast exchange between an axially symmetric form and a higher energy form. There are increasing numbers of examples of proteins that populate excited-state conformations related to the crystal structure in solution[19] and may reconcile instances where the solution and crystal structures of a given protein appear to differ. In the present case, errors in the experimentally derived values of $\Delta\omega$, together with uncertainties in the theoretical values derived from density functional theory, preclude a firm assignment of the excited state to that observed in the crystal structure. However, data obtained in the present study suggest that the excited state is populated ∼10%, and thus it should be possible to obtain evidence for the nature of this state by independent methods, and this work is in progress.

The binding of the bivalent ligand P^k dimer straddles adjacent monomers[7] and suppresses the conformational equilibrium but with a substantial entropic cost to binding. Under the assumption that a second P^k dimer molecule bound to the homopentamer does not interact with the first, an estimate of this entropic cost can be obtained from the difference between $T\Delta S_1°$ (-103.6 kJ/mol) and $T\Delta S_2°$ (-35.1 kJ/mol) derived by fitting ITC data to the sequential model of binding as described above, i.e.,

(18) Koradi, R.; Billeter, M.; Wuthrich, K. *J. Mol. Graphics* **1996**, *14*, 51.
(19) Lukin, J. A.; Kontaxis, G.; Simplaceanu, V.; Yuan, Y.; Bax, A.; Ho, C. *Proc. Natl. Acad. Sci. U.S.A.* **2003**, *100*, 517−520.

$T\Delta\Delta S = -68.5$ kJ/mol at 45 °C. This contribution to the thermodynamics of binding is a major factor in the unexpectedly low affinity of the first molecule of P^k dimer to VTB. However, the more favorable entropy of binding of the second molecule of P^k dimer is offset by a less favorable enthalpy of binding, resulting in a similar affinity. Nonetheless, these thermodynamics indicate positive entropic cooperativity in a polyvalent system, which has not previously been observed.[20] The observed affinity of P^k dimer contrasts with the much higher affinity for a decavalent inhibitor (starfish).[21] Thus, valency greater than 2 appears to be a prerequisite for high-affinity inhibition of the action of this toxin, due in part to the large unfavorable entropic cost of straddling adjacent monomers resulting from the novel intersubunit motions described herein.

(20) Mammen, M.; Choi, S.-K.; Whitesides, G. M. *Angew. Chem., Int. Ed.* **1998**, *37*, 2754−2794.
(21) Kitov, P. I.; Sadowska, J. M.; Mulvey, G.; Armstrong, G. D.; Ling, H.; Pannu, N. S.; Read, R. J.; Bundle, D. R. *Nature* **2000**, *403*, 669−672.